

# Design of a Load-based DRX Scheme for Non-Real-Time Traffic in LTE

Chun-Chuan Yang, \*Jeng-Yueng Chen, Yi-Ting Mai, and Ching-Hsiang Liang

**Abstract**—In this paper, a revised version of the authors' previously proposed power saving scheme for IEEE 802.16 is proposed to be applied in LTE. The proposed scheme namely LTE-LBPS-Aggr treats the traffic of all UEs as a single flow, estimates the input load by traffic measurement and the channel capacity by CQI reports, calculates the length of the sleep cycle, and notifies all UEs of the next radio-on time for receiving data. Simulation study shows that the proposed scheme outperforms the standard DRX mechanism in terms of the power saving efficiency and the delay performance.

**Index Terms**—LTE, DRX, Power Saving, LBPS

## I. INTRODUCTION

WITH the increasing popularity of all sorts of mobile devices and Apps, modern life is being brought into a new era of mobile communications in recent years. To address the intense demand, the wireless technology for the fourth generation (4G) [1] of mobile broadband communications is standardized. 4G candidate systems including Mobile WiMAX [2] and LTE (Long Term Evolution) [3-4] are commercially deployed. LTE standard is defined and supported by all major players in the telecommunication industry and is backward compatible with GSM/UMTS cellular systems, which makes LTE deployment easier than Mobile WiMAX, giving LTE benefit over its competitors in 4G market.

Although based on GSM/EDGE and UMTS/HSPA network technologies, both the core network (Evolved Packet Core, EPC) and the radio access (Evolved Universal Terrestrial Radio Access Network, E-UTRAN) in LTE are fully packet-switched, rather than following the circuit-switched model of earlier systems. LTE is designed to work with a variety of different bandwidths and to deliver a peak data rate of 100 Mbps in the downlink and 50 Mbps in the uplink. The enhanced version of LTE, namely LTE-Advanced (LTE-A), is designed with advanced features to deliver a peak data rate of 1000 Mbps in the downlink, and 500 Mbps in the uplink. The specifications for LTE produced by the Third Generation Partnership Project (3GPP) are organized into releases, each of which contains a stable and clearly defined set of features. LTE was first introduced in Release 8 [3], and initial enhancements were included in Release 9. The extra capabilities required for LTE-A were specified in Release 10 [4]. As the specification of Release 11 of the LTE standards

is approaching its completion, 3GPP is gradually moving its focus toward the next major step in the evolution of LTE (Release 12).

One of the major issues in mobile communications is power saving/management at the user side as well as at the network side. Power saving at the network side creates the benefit of energy cost reduction, but the user side is more critical since the user device is usually battery-powered and the length of the operational time in communications is always a main focus. Discontinuous Reception mode (DRX) [5-6] is supported to conserve the power of the mobile terminal namely the User Equipment (UE) in LTE. The UE powers down most of its circuitry in DRX when there are no packets to be transmitted or received. During this time, the UE listens to the downlink (DL) occasionally and may not keep in sync with uplink (UL) transmission depending on its RRC (Radio Resource Control) state. There are additional advantages in using DRX, such as radio link resource saving on both UL and DL to increase system capacity.

The authors have been working on the issue of power saving in IEEE 802.16 for some years. The idea of Load-Based Power Saving (LBPS) and associated schemes were proposed to adaptively schedule the sleep (radio off) time of the user device for the current network load [7]. Extension of LBPS to integrate the user side and the network side in sleep scheduling was also proposed [8]. In this paper, a revised scheme of LBPS applying to LTE DRX is proposed. Simulation study shows that the proposed scheme can adapt to the fluctuated system capacity as well as the input load and achieve high power saving efficiency. The remainder of the paper is organized as follows. In section II, a survey of the standard DRX in LTE, DRX related work, and our previous work of LBPS in IEEE 802.16 is presented in section II. Proposed LBPS scheme for LTE is presented in section III. Performance evaluation is presented in section IV. Finally, section V concludes this paper.

## II. RELATED WORK

### A. LTE DRX

In LTE DRX mode can be enabled in both of the states of the radio link between the UE and the base station (called eNodeB or eNB): *RRC\_idle* and *RRC\_connected*. In the *RRC\_idle* state, the UE is registered with the network but does not have an active session, and the UE can be paged for

Manuscript received Dec. 08, 2013; revised Dec. 08, 2013. This work was supported in part by the National Science Council, Taiwan, under grant no. NSC 102-2221-E-260-013.

Chun-Chuan Yang is with Dept. of Computer Science and Information Engineering, National Chi Nan University, Taiwan (e-mail: ccyang@csie.ncnu.edu.tw).

Jeng-Yueng Chen is with Dept. of Information & Networking Technology, Hsiuping Univ. of Science & Technology, Taiwan (e-mail: jychen@mail.hust.edu.tw, Corresponding author)

Yi-Ting Mai is with Dept. of Information & Networking Technology, Hsiuping Univ. of Science & Technology, Taiwan (wkb@wkb.idv.tw).

Ching-Hsiang Liang is with Dept. of Computer Science and Information Engineering, National Chi Nan University, Taiwan.

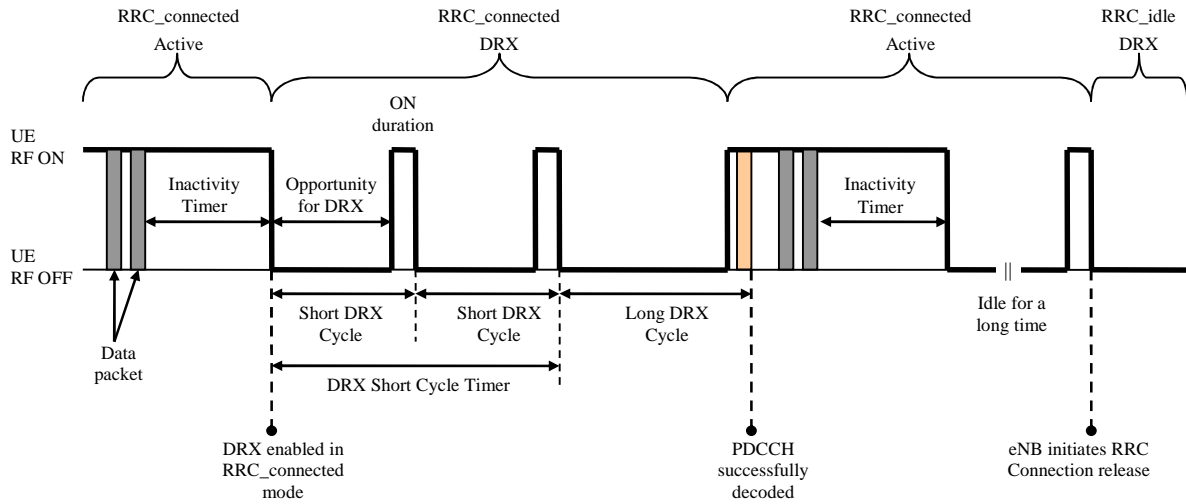


Figure 1. Illustration of LTE DRX

DL traffic. In the *RRC\_connected* state DRX mode is enabled during the idle periods during the packet arrival process. When there are no outstanding packets to be transmitted or received, eNB or UE may initiate the DRX mode.

As illustrated in Figure 1, a DRX cycle consists of an “*Opportunity for DRX period*” (radio off) during which the UE can skip reception of DL channels and an “*ON duration*” (radio on) during which the UE should monitor the *physical downlink control channel (PDCCH)* to identify DL data. The *inactivity timer* is used to trigger the start of a DRX cycle in the *RRC\_connected* state. The parameterization of the DRX cycle involves a trade-off between battery saving and latency. A long *Opportunity for DRX period* is beneficial for lengthening the UE’s battery life. On the other hand, a shorter DRX period is better for faster response. Therefore, two DRX cycles, namely *Short DRX Cycle* and *Long DRX Cycle*, can be configured for each UE. The transition between the *Short DRX Cycle* and the *Long DRX Cycle* can be controlled by the *DRX Short Cycle Timer* or by explicit commands from eNB.

Analytical models for performance evaluation of the DRX operation in terms of power saving efficiency and transmission delay were proposed in the literature [9-10]. Heuristic mechanisms for adjusting the value of the inactivity timer based on *CQI (Channel Quality Indicator)* report was proposed in [11], in which higher CQI makes shorter inactivity timer for better system utility. Impact of the length of *TTI (Time Transmission Interval)* on power saving efficiency and access delay was investigated in [12]. Optimization of the two conflicting performance metrics, power saving and access delay, was addressed in [13-14].

### B. Previous work of LBPS

The objective of LBPS is to adaptively adjust sleep window size of each *MSS (Mobile Subscriber Station)* to better fit in current traffic load by traffic measurement. The BS in LBPS needs to estimate the current load for each MSS (denoted by packets per time frame) by collecting and exponentially averaging the samples of load measure as in *TCP Round-Trip Time (RTT)* estimation. For presentation purpose, only downlink traffic is considered in this paper, although uplink traffic can also be integrated into LBPS schemes via some information exchange mechanism between the BS and MSSs. LBPS sets a target threshold of data accumulation in the buffer for an MSS and dynamically

calculates its next sleep window size. In this way, LBPS can adapt to different traffic loads and still achieves a proper level of powering saving. The basic version of LBPS, *LBPS-Aggr*, in which all the traffic in the network is treated as an aggregate flow in calculating the size of the sleep window. In *LBPS-Aggr*, the traffic arrival process is assumed to be Poisson, and data accumulation under load  $\lambda$  in a time frame is calculated by the following equation:

$$Prob [i \text{ packet arrivals in a time frame}] = \frac{e^{-\lambda T} (\lambda T)^i}{i!},$$

where  $T$  is the length of a time frame.

The threshold of data accumulation is denoted by *Data\_TH* (packets), which is practically set as the capacity of a time frame. The probability of data accumulation exceeding *Data\_TH* packets over  $K$  time frames in a row can be calculated as follows:

$$\begin{aligned} P_{Acc}(K, Data\_TH) &\equiv \\ Prob [\# \text{ of packet arrivals in } K \text{ time frames} > Data\_TH] & \\ = \sum_{i=Data\_TH+1}^{\infty} \frac{e^{-\lambda KT} (\lambda KT)^i}{i!} & \\ = 1 - \sum_{i=0}^{Data\_TH} \frac{e^{-\lambda KT} (\lambda KT)^i}{i!} & \end{aligned}$$

The number of time frames (including the current awake time frame) before the next awake time frame for an MSS is calculated as the smallest value of  $K$  such that  $P_{Acc}(K, Data\_TH)$  is higher than a predefined probability threshold denoted by *Prob\_TH*. That is,

$$\begin{aligned} \text{The length of one awake-and-sleep cycle} & \\ \equiv LengthAwkSlpCyl(\lambda, Data\_TH) &\equiv K^* \\ = Min\{K \mid P_{Acc}(K, Data\_TH) \geq Prob\_TH\}, & \text{ where an} \\ \text{awake-and-sleep cycle is composed of the current} & \\ \text{awake time frame and the following sleep window.} & \end{aligned}$$

The size of the sleep window in a cycle is therefore  $K^*-1$ , which is sent by the BS to the currently awake MSSs to prepare for entering the sleep mode.

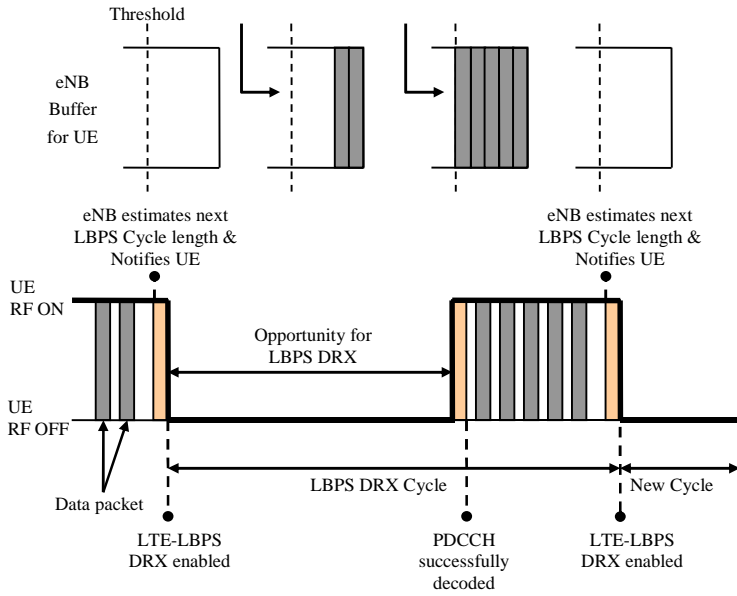


Figure 2. Illustration of LTE-LBPS

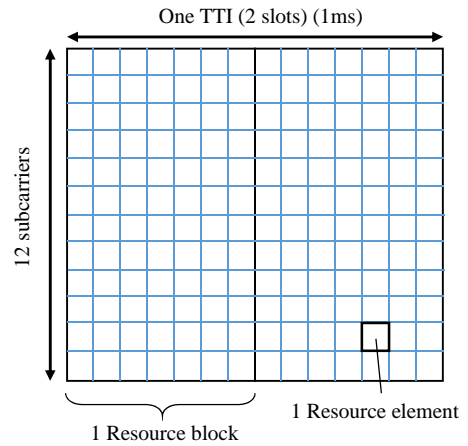


Figure 3. Basic time-frequency resource structure of LTE TTI

Improved mechanisms of *LBPS-Aggr* were also proposed in our previous work by elaborately grouping MSSs in sleep scheduling for better power saving efficiency, which are not surveyed in this paper since the proposed LBPS DRX scheme in LTE is mainly based on *LBPS-Aggr*.

### III. LTE-LBPS

#### A. Basic idea

The previous work of *LBPS-Aggr* was designed for IEEE 802.16. Applying *LBPS-Aggr* to LTE requires proper addressing the features of LTE, which are discussed as follows:

- (1) As illustrated in Figure 3, the basic time unit for packet scheduling and transmission in LTE is called a *TTI (Transmission Time Interval)* with length of 1ms. Thus, TTI is the time unit for LBPS to estimate the length of the sleep cycle in LTE. In each TTI, a scheduling decision is made where each scheduled UE is assigned a certain amount of radio resources in the time and frequency domain. In the time domain, a TTI is split into two 0.5ms slots. Each slot comprises 7 OFDM symbols in the case of the normal cyclic prefix length. In the frequency domain, resources are grouped in units of 12 subcarriers, such that one unit of 12 subcarriers for a duration of one slot is called a *Resource Block (RB)*, which is the smallest element of resource allocation. The smallest unit of resource is the *Resource Element (RE)*, which consists of one subcarrier for a duration of one OFDM symbol. Therefore, an RB is comprised of 84 (7x12) REs in the case of the normal cyclic prefix length.
- (2) In order for LBPS to estimate the awake TTI in LTE for a given threshold of data accumulation (*DATA\_TH*), it is necessary to estimate the current traffic load as well as the channel capacity. In our previous work, the channel capacity is assumed to be static, which should be revised for LTE. In LTE, eNB typically selects the modulation scheme and code rate depending on a prediction of the DL channel condition, which is according to the *Channel Quality Indicator (CQI)* feedback transmitted by the UE.

3GPP gives a table of reference for efficiency of each CQI index as shown in Table 1. The estimation of the channel capacity of LBPS in LTE is therefore based on the CQI report from the UE and the corresponding efficiency value in Table 1. Moreover, since LTE physical control channels (such as PDCCH, PCFICH, PHICH) also make use of the REs in the TTI, estimation of the capacity for the user data should exclude the REs reserved for the control channels.

Table 1. CQI table by 3GPP

CQI index	Modulation	Approximate code rate	Efficiency (bits/RE)
0	No Tx	--	--
1	QPSK	0.076	0.1523
2	QPSK	0.12	0.2344
3	QPSK	0.19	0.3770
4	QPSK	0.3	0.6016
5	QPSK	0.44	0.8770
6	QPSK	0.59	1.1758
7	16QAM	0.37	1.4766
8	16QAM	0.48	1.9141
9	16QAM	0.6	2.4063
10	64QAM	0.45	2.7305
11	64QAM	0.55	3.3223
12	64QAM	0.65	3.9023
13	64QAM	0.75	4.5234
14	64QAM	0.85	5.1152
15	64QAM	0.93	5.5547

In this paper, the revised version of *LBPS-Aggr* for LTE is named *LTE-LBPS-Aggr*. An overview of the proposed scheme is illustrated in Figure 4.

#### B. LTE-LBPS-Aggr

Downlink traffic to all UEs is treated as a single traffic flow in *LTE-LBPS-Aggr*, but the eNB estimates the traffic load and the channel capacity for each UE respectively. As in our previous work, estimation of the traffic load for a UE is based on traffic measurement and is calculated by exponentially averaging the samples of load measure. On the other hand, estimation of the channel capacity depends on the CQI reports from a UE, meaning that different UEs would have different views of the channel capacity. Estimation of the channel capacity for a UE also requires to address the type of CQI report. Two types of CQI reports are addressed in this paper:

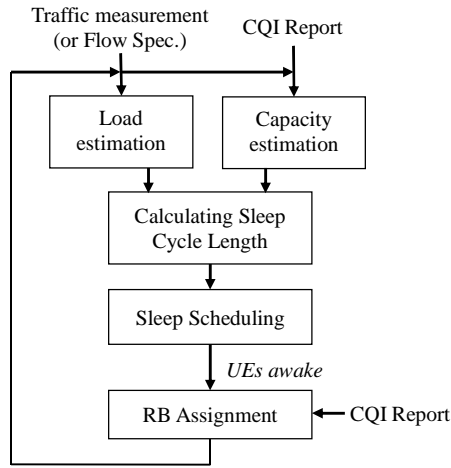


Figure 4. Overview of LTE-LBPS-Aggr

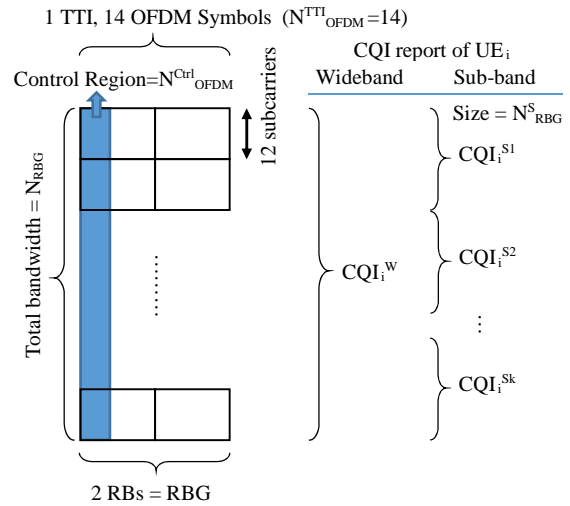


Figure 5. Notations used in capacity estimation

*Wideband* report and *Full-Sub-band* report. In *Wideband* report, the UE reports one wideband CQI value for the whole system bandwidth. In *Full-Sub-band* report, in addition to the wideband CQI value, the UE reports a CQI value for each sub-band with system-defined sub-band size. Notations used in estimation of the channel capacity for  $UE_i$  are defined as follows and also illustrated in Figure 5.

$N_{OFDM}^{TTI}$ : The number of OFDM symbols (REs) in a TTI, which is 14 in the case of the normal cyclic prefix length.

$N_{OFDM}^{Ctrl}$ : The number of OFDM symbols used by the control channels in a TTI.

$N_{OFDM}^{Resv}$ : The number of OFDM symbols reserved for reference signals in a TTI of 12 subcarriers.

Note that the two RBs in a TTI of 12 subcarriers are called a *Resource Block Group (RBG)* in the paper. Therefore, the number of REs for the user data in an RBG, denoted by  $N_{RE}^{TTI}$ , is calculated as follows.

$$N_{RE}^{TTI} = (N_{OFDM}^{TTI} - N_{OFDM}^{Ctrl}) \times 12 \text{ (subcarriers)} - N_{OFDM}^{Resv}$$

For the case of *Wideband* report, the channel capacity estimated for  $UE_i$  in a TTI, denoted by  $C_i^W$ , are calculated as follows.

$C_i^W = N_{RE}^{TTI} \times \text{Eff}(CQI_i^W) \times N_{RBG}$ , where the function of  $\text{Eff}(CQI_i^W)$  returns the efficiency value for the given wideband CQI value  $CQI_i^W$  according to Table 1, and  $N_{RBG}$  is the total number of RBG in the system.

For the case of *Full-Sub-band* report, the channel capacity estimated for  $UE_i$  in a TTI, denoted by  $C_i^S$ , are calculated as follows.

$$C_i^S = \sum_{\forall S_k} (N_{RE}^{TTI} \times \text{Eff}(CQI_i^{S_k}) \times N_{RBG}^S), \text{ where } CQI_i^{S_k} \text{ is the}$$

CQI value for sub-band  $S_k$ , and  $N_{RBG}^S$  is the number of RBG in a sub-band.

As in the estimation of the traffic load for a UE, the estimation of the current channel capacity, denoted by  $C_i$ , is calculated by exponentially averaging the samples of each calculation. Since all UEs are treated as a group, the channel capacity for all UEs is calculated by combing the channel capacity estimated for individual UE with the ratio of the UE's traffic load in the group as follows.

*Channel capacity for all UEs (bits/TTI) =*

$$C_{System} = \sum_{\forall UE_i} (C_i \frac{\lambda_i}{\lambda}), \text{ where } \lambda \text{ is the total DL load and } \lambda_i \text{ is the current load of } UE_i.$$

The threshold of data accumulation in LTE-LBPS-Aggr is set as a percentage ( $\alpha$ ) of the capacity for the user data in a TTI, that is  $DATA\_TH = C_{System} \times \alpha$ , in which  $\alpha$  is set as 80% in the simulation in order to avoid the probability of data overflow in a TTI. Calculation of the length of one sleep-and-awake cycle (in units of TTI) is the same as in our previous work presented in Section II-B. The eNB notifies all UEs of the cycle length via DRX signaling, and all UEs enter DRX mode until the awake TTI for DL reception as illustrated in Figure 2.

#### IV. PERFORMANCE EVALUATION

Simulation study is conducted to evaluate the performance of LTE-LBPS-Aggr. Simulation parameters are listed in Table 2. In order to simulate different cases of channel quality, three types of UEs are defined. CQI values for each sub-band in an *H-type* (high-quality) UE ranges from 10 to 15 by modulation of 64QAM. *M-type's* (medium quality) CQI ranges from 7 to 9 by modulation of 16QAM. *L-type's* (low quality) CQI ranges from 1 to 6 by modulation of QPSK. In the simulation, the average channel capacity of an *H-type* UE is 56.19Mbps (Wideband report) and 58.38Mbps (Full-Sub-band report). *M-type* is 24.41Mbps (Wideband report) and 26.86Mbps (Full-Sub-band report). *L-type* is 5.43Mbps (Wideband report) and 6.22Mbps (Full-Sub-band report). The total input load (denoted by  $\lambda$  Mbps) in the simulation depends on the type of UEs in the network, and the utilization factors  $\rho_{WB}$  and  $\rho_{SB}$  are defined as the ratio of the total input load over the average channel capacity for the case of Wideband report (WB) and

Full-Sub-band report (SB), respectively. Two contrast schemes (DRX1 and DRX2) based on the standard DRX operation are also simulated. Parameters for DRX1 and DRX2 are listed in Table 2. Two performance criteria are investigated and presented in this paper: *Power Saving Efficiency* (denoted by *PSE*) and *Average Delay* (denoted by *AvgD*), in which *PSE* is defined as the ratio of radio-off time.

Table 2. Simulation Parameters

Channel capacity related	$N_{OFDM}^{TTI} = 14, N_{OFDM}^{Ctrl} = 2$ $N_{OFDM}^{Resv} = 0$ $N_{RBG} = 100, N_{RBG}^S = 8$
# UE	12 (equal load)
Type of UE	<i>H-type</i> : CQI 11~15 <i>M-type</i> : CQI 6~10 <i>L-type</i> : CQI 1~5
Packet Size	799 bits
<i>DATA_TH</i>	$C_{System} \times \alpha, \alpha = 0.8$
<i>Prob_TH</i>	0.8
Contrast scheme DRX1	On duration = 1ms Inactivity timer = 10ms Short DRX Cycle = 80ms Short Cycle timer = 2 Long DRX Cycle = 320ms
Contrast scheme DRX2	On duration = 1ms Inactivity timer = 10ms Short DRX Cycle = 160ms Short Cycle timer = 2 Long DRX Cycle = 640ms

Figure 6 ~ Figure 8 show the result of *PSE* for each of the following three input cases: all *H-type* UEs, all *M-type* UEs, and all *L-type* UEs. The corresponding result of *AvgD* for each UE case is displayed in Figure 9 ~ Figure 11, respectively. Note that in the figures there are three rows of index for the *x-axis*. The upper row is the input load  $\lambda$  in Mbps, the middle row is the utilization factor  $\rho_{WB}$  for the case of Wideband report, and the lower row is the utilization factor  $\rho_{SB}$  for the case of Full-Sub-band report. Following observations can be made from the figures.

- (1) The scheme of LTE-LBPS-Aggr can adapt to different input load and channel capacity and outperform DRX1 and DRX2 in terms of *PSE* and *AvgD*, except in the case of *All-L type* UEs in Figure 8. Since in the case of *All-L type* UEs, the arrival rate of packet with fixed size (799 bits) is pretty low even in high utilization, triggering the inactivity timer of DRX1 and DRX2 to expire and achieve higher *PSE* in the cost of unacceptable high *AvgD* in Figure 11.
- (2) *PSE* of Full-Sub-band report is slightly higher than Wideband report in all cases for the proposed LTE-LBPS-Aggr. The reason is the channel capacity by Full-Sub-band report is a little bit higher than the channel capacity by Wideband report, making the utilization factor of  $\rho_{SB}$  a little bit smaller than  $\rho_{WB}$ , which results in longer sleep cycle length for the case of Full-Sub-band report.

## V. CONCLUSION

As a promising technology for 4G mobile communications, LTE has attracted more and more attention in the literature. An important research issue in LTE is power saving at the user side of UE, which is based on the idea of DRX specified in the standard. Based on the authors' previous work of Load-Based Power Saving (LBPS) in IEEE 802.16, a revised version of LBPS scheme namely LTE-LBPS-Aggr is proposed in the paper. LTE-LBPS-Aggr treats the traffic of all UEs as an aggregate flow and synchronizes the sleep schedule of all UEs. Based on the estimation of the input load by traffic measurement and the estimation of the channel quality by CQI reports, LTE-LBPS-Aggr calculates the proper length of a sleep cycle and notifies all UEs of the time for turning on radio to receive data. Simulation study shows that the power saving efficiency as well as the delay performance of the proposed scheme are better than the standard DRX mechanism. Future work of the research is to incorporate more sophisticated LBPS scheme in LTE to get rid of the constraint of synchronous sleep schedule in LTE-LBPS-Aggr, which can also reduce the overload of PDCCH to notify all UEs of the coming data at the same time.

## REFERENCES

- [1] U. Varshney, "4G Wireless Networks," IT Professional, vol. 14, issue 5, Oct. 2012, pp. 34-39.
- [2] D. Pareit, B. Lannoo, I. Moerman, and P. Demeester, "The History of WiMAX: A Complete Survey of the Evolution in Certification and Standardization for IEEE 802.16 and WiMAX," IEEE Communications Surveys & Tutorials, vol. 14, no. 4, pp. 1183-1211, 2012.
- [3] 3GPP TS 36.300, "Evolved Universal Terrestrial Radio Access (E-UTRA) and Evolved Universal Terrestrial Radio Access Network (E-UTRAN)," Rel. 8, v8.5.0, May 2008.
- [4] 3GPP TS 36.300, "Evolved Universal Terrestrial Radio Access (E-UTRA) and Evolved Universal Terrestrial Radio Access Network (E-UTRAN)," Rel. 10, v10.3.0, Mar. 2011.
- [5] 3GPP Contribution, Nokia, R2-071285, "DRX parameters in LTE", March 2007.
- [6] C. Bontu, and E. Illidge, "DRX Mechanism for Power Saving in LTE," IEEE Communications Magazine, vol. 47, no. 6, June 2009, pp. 48-55.
- [7] C. C. Yang, Y. T. Mai, J. Y. Chen, Y. S. Shen, and Y. C. Kuo, "LBPS: Load-based Power Saving in the IEEE 802.16e Network," Computers and Electrical Engineering, vol. 38, no. 4, Jul. 2012, pp. 91-905.
- [8] C. C. Yang, Y. T. Mai, J. Y. Chen, and Y. C. Kuo, "Integrated Load-Based Power Saving for BS and MSS in the IEEE 802.16e Network," Wireless Communications and Mobile Computing, 18 Mar. 2013. DOI: 10.1002/wcm.2365
- [9] S. Jin, and D. Qiao, "Numerical Analysis of the Power Saving in 3GPP LTE Advanced Wireless Networks," IEEE Transactions on Vehicular Technology, volume 61, issue 4, May 2012, pp. 1779-1785.
- [10] S. Fowler, R. S. Bhamber, and A. Mellouk, "Analysis of Adjustable and Fixed DRX Mechanism for Power Saving in LTE/LTE-Advanced," Proceedings, IEEE International Conference on Communications (ICC), 2012, pp. 1964-1969.
- [11] S. Gao, H. Tian, J. Zhu, and L. Chen, "A More Power-Efficient Adaptive Discontinuous Reception Mechanism in LTE," Proceedings, IEEE Vehicular Technology Conference (VTC Fall), September 2011, pp. 1-5.
- [12] S. Fowler, "Study on Power Saving Based on Radio Frame in LTE Wireless Communication System Using DRX," Proceedings, IEEE GLOBECOM Workshops, 2011, pp. 1062-1066.
- [13] Y.-P. Yu, and K.-T. Feng, "Traffic-Based DRX Cycles Adjustment Scheme for 3GPP LTE Systems," Proceedings, IEEE Vehicular Technology Conference (VTC Spring), May 2012, pp. 1-5.
- [14] A. T. Koc, S. C. Jha, R. Vannithamby, and M. Torlak, "Optimizing DRX Configuration to Improve Battery Power Saving and Latency of Active Mobile Applications Over LTE-A network," Proceedings, IEEE Wireless Communications and Networking Conference (WCNC), 2013, pp. 568-573.

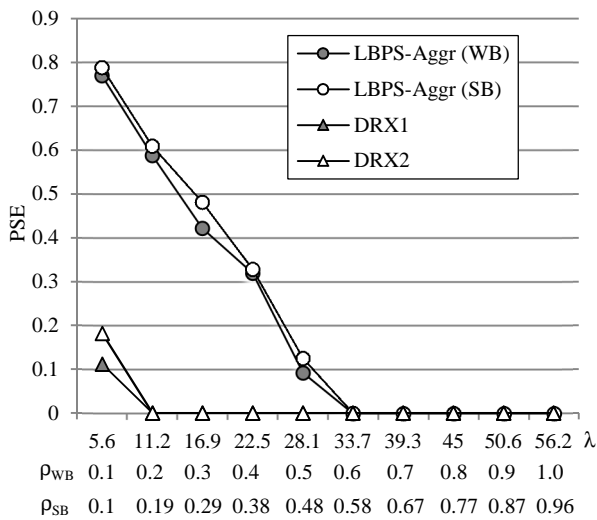


Figure 6. PSE in the case of All-H UEs

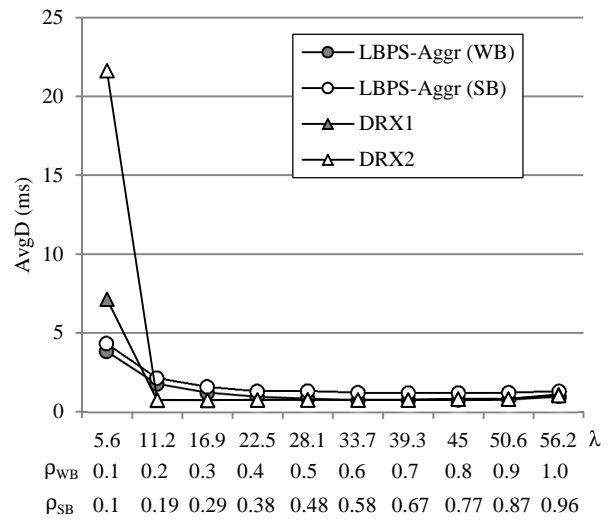


Figure 9. AvgD in the case of All-H UEs

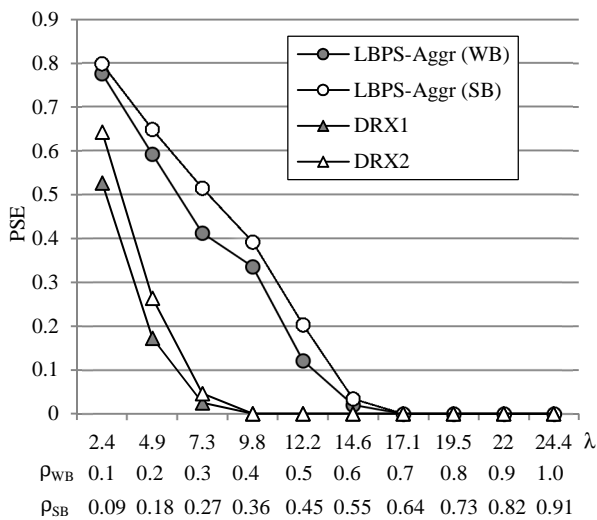


Figure 7. PSE in the case of All-M UEs

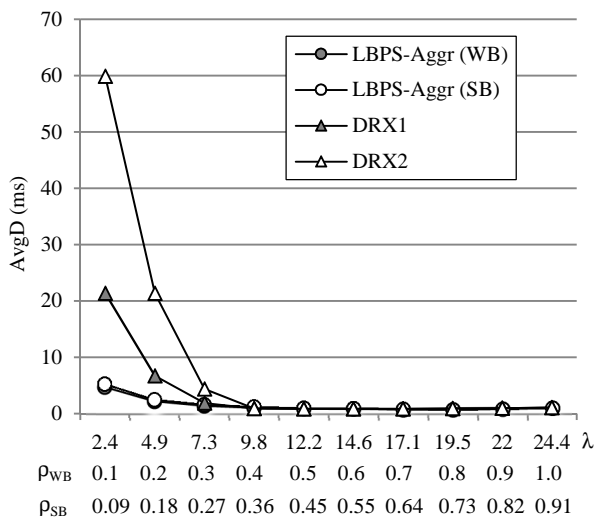


Figure 10. AvgD in the case of All-M UEs

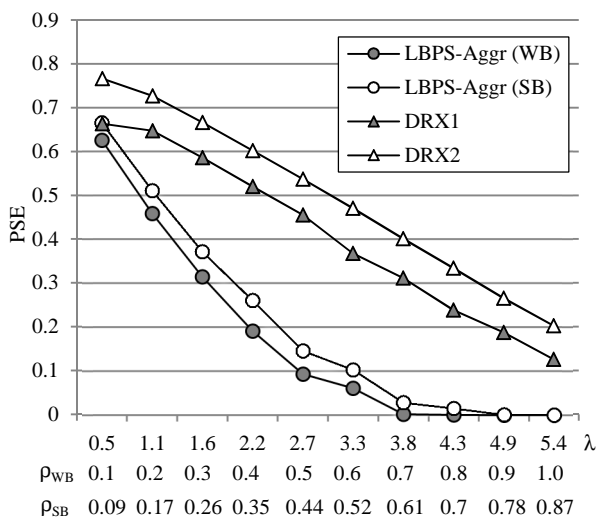


Figure 8. PSE in the case of All-L UEs

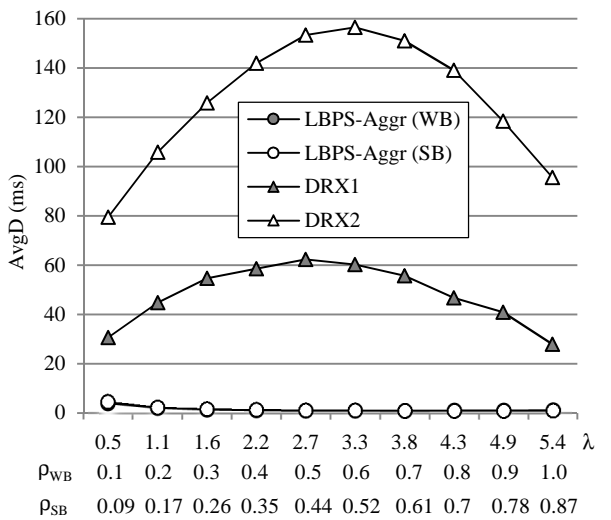


Figure 11. AvgD in the case of All-L UEs